Propulsion of flexible polymer structures in a rotating magnetic field

2009 J. Phys.: Condens. Matter 21 204110

(http://iopscience.iop.org/0953-8984/21/20/204110)

IOP Publishing Journal of Physics: Condensed Matter

J. Phys.: Condens. Matter **21** (2009) 204110 (8pp) doi:10.1088/0953-8984/21/20/204110

Propulsion of flexible polymer structures in a rotating magnetic field

Piotr Garstecki[1,6], Pietro Tierno[2,3], Douglas B Weibel[4], Francesc Sagués[2,3] and George M Whitesides[5]

[1] Institute of Physical Chemistry, Polish Academy of Sciences, Kasprzaka 44/52, 01-224, Warsaw, Poland
[2] Department de Química Física, Universitat de Barcelona, Martí i Franquès 1 Barcelona, 08028, Spain
[3] Institut de Nanociència i Nanotecnologia de la UB (IN^{2}UB), Universitat de Barcelona, Barcelona, Spain
[4] Department of Biochemistry, University of Wisconsin-Madison, 433 Babcock Drive, Madison, WI 53706, USA
[5] Department of Chemistry and Chemical Biology, Harvard University, 12 Oxford Street, Cambridge, MA 02138, USA

E-mail: garst@ichf.edu.pl

Received 8 December 2008, in final form 11 February 2009
Published 21 April 2009
Online at stacks.iop.org/JPhysCM/21/204110

Abstract
We demonstrate a new concept for the propulsions of abiological structures at low Reynolds numbers. The approach is based on the design of flexible, planar polymer structures with a permanent magnetic moment. In the presence of an external, uniform, rotating magnetic field these structures deform into three-dimensional shapes that have helical symmetry and translate linearly through fluids at Re between 10^{-1} and 10. The mechanism for the motility of these structures involves reversible deformation that breaks their planar symmetry and generates propulsion. These elastic propellers resemble microorganisms that use rotational mechanisms based on flagella and cilia for their motility in fluids at low Re.

M This article features online multimedia enhancements

(Some figures in this article are in colour only in the electronic version)

1. Introduction

This paper describes a new concept for artificial, externally powered elastic objects which 'swim' in viscous fluids using a rotational mechanism for their motility. The approach is based on the design and fabrication of flexible planar structures that deform into three-dimensional (3D) shapes that possess helical symmetry (i.e. are chiral). These rotating helical structures exhibit net movement at low and medium Reynolds numbers (Re). For simplicity, and because their movement is reminiscent of microorganisms that use flagella and cilia for motility in fluids, we refer to these structures as 'swimmers'. These objects are fabricated using single step soft lithography. We create molds embossed in a layer of elastomer (poly(dimethylsiloxane), (PDMS)), fill the indentations with PDMS prepolymer admixed with magnetic nanoparticles (i.e. magnetite), and cure the polymer in a constant magnetic field to create swimmers with a permanent magnetic moment. When immersed in a viscous fluid in the presence of an external, rotating magnetic field, the swimmers rotate around their long axis and as a result of the viscous torque that counteracts the rotation, they deform into a chiral shape. When the magnetic field is turned off, the objects stop rotating and relax back to their equilibrium, non-distorted shape.

Microorganisms translate through fluids at low Re [1–5]. In response to the physics of fluids at this length scale [6], microbial cells have evolved sophisticated mechanisms of motility, including those based on the movement of intracellular and extracellular organelles (e.g. flagella and cilia). One of the best-studied examples of microbial motility

[6] Author to whom any correspondence should be addressed.

is the bacterium *Escherichia coli*. Cells of *E. coli* translate through fluids by rotating their helical flagella (∼4–5 per cell) at a frequency of 100–200 Hz using the biological equivalent of a rotary motor [7]. When all of the motors rotate in the same direction—counter-clockwise, when visualized from behind the cell—the flagella bundle and rotate together, and the work exerted by the bundle on the fluid propels cells at a velocity approaching 20–25 μm s^{-1}. The torque generated by the rotating bundle of flagella is balanced by the viscous drag from the counter rotation of the cell body around its long axis at a frequency of ∼10 Hz, which is in part responsible for the behavior of cells in the proximity of surfaces and interfaces [8–10]. Other examples of single-celled model organisms that rotate during their movement in fluids using external organelles include algae (e.g. *Chlamydomonas reinhardtii*) and protozoa (e.g. *Paramecium tetraurelia*). We were interested in testing whether a similar design concept—that is, the rotation of a helical object at low *Re*—may provide a feasible mechanism for the autonomous movement of synthetic, abiological objects [11–13]. Although the swimmers described in this paper are powered by an external, rotating magnetic field, we refer to their motion as 'self-propulsion' because the field produces only rotation, while net movement emerges from the deformation of the appropriately designed elastic object.

Several different mechanisms have been developed for the autonomous movement and actuation of nano- [14, 15], micro- [16–18], and meso-scale [19, 20] objects suspended in fluids. Applications of these objects include the transport of sensors and the study of complexity and emergent behavior in systems containing many self-propelled components. One approach for autonomous movement is based on the conversion of chemical energy to mechanical work [21–23, 14, 24–28]. Strategies for propelling micron-scale particles through fluids by converting electrical energy into mechanical work have also been described. For example, Dreyfus *et al* have described a remarkable 'engine' that mimics eukaryotic flagella and is based on a chain of DNA linked paramagnetic colloids that is attached to a particle and can be actuated by an oscillating magnetic field [16]. Other examples of biologically relevant mechanisms for moving micron and meso-scale objects in fluids have integrated live unicellular organisms into synthetic structures and have harnessed their motility [29–33].

In this paper we explore a bio-inspired mechanism for moving meso-scale ferromagnetic polymeric structures by rotating and deforming them into helical shapes in a rotating magnetic field. In figure 1 we show a large scale (length equal to 13 mm), prototype elastic swimmer and three consecutive snapshots of the swimming of a collection of these magnetic 'fish' in a Petri dish filled with glycerine and positioned above a rotating bar magnet. The behavior of these swimmers is arresting: the video of their motion is strikingly similar to the appearance of a collection of fish in a pond, when viewed from above (see video 1 in the supplementary information available at stacks.iop.org/JPhysCM/21/204110). As we discuss it in detail in this paper, the swimmers swim because the viscous torque that opposes their rotation deforms these elastic objects into chiral shapes that 'screw' through the viscous fluid.

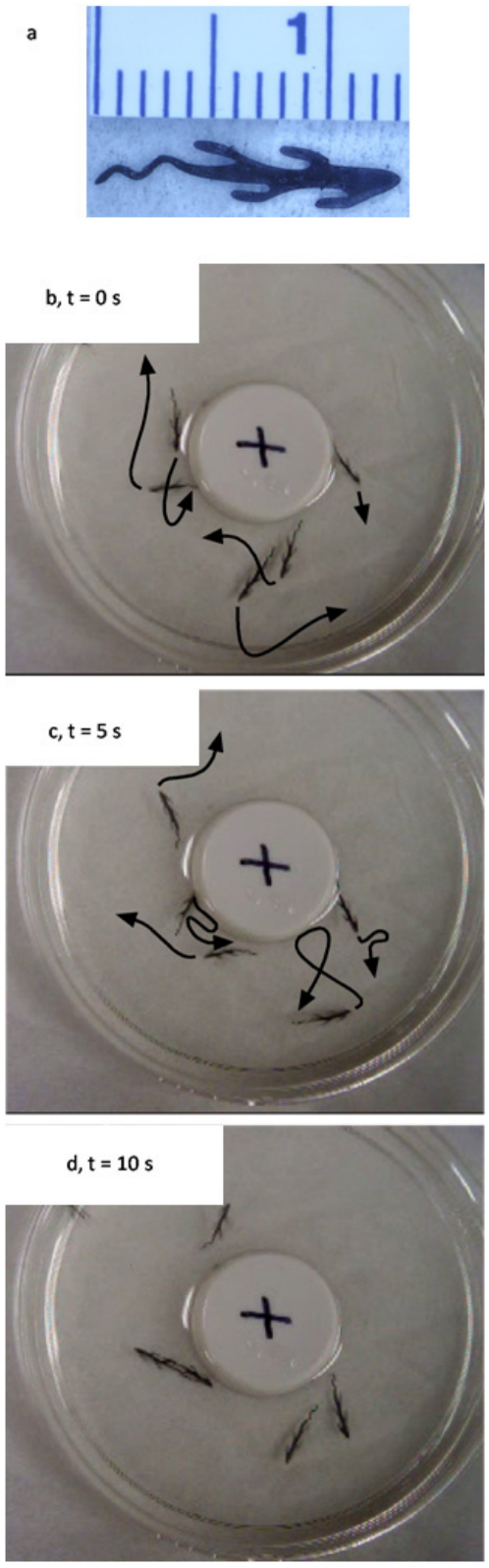

Figure 1. (a) A photograph of an elastic swimmer made of poly(dimethylosiloxane) doped with ferromagnetic powder and cured in the presence of magnetic field. The photographs (b)–(d) show the motion of a collection of such swimmers in a Petri dish filled with glycerine and positioned on a magnetic stir plate. The cross (×) on the plastic cylinder in the middle of the Petri dish marks the axis of rotation of the bar magnet; the cylinder prevents the swimmers from entering the central region of the dish and from rotating about this vertical axis.

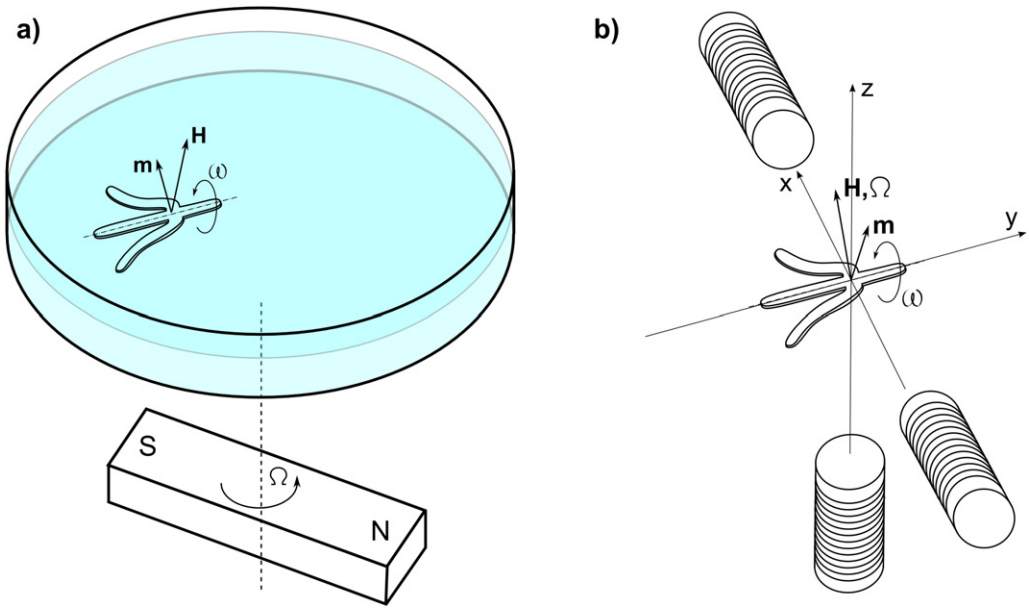

Figure 2. Cartoons depicting the rotating magnetic field systems that were used in this study. (a) A magnetic stir plate with a rotating magnet. The swimmer is immersed in a fluid in a Petri dish. In spite of the fact that the axis of rotation of the magnet is perpendicular to the plane of the dish, there is a component of the magnetic field that rotates in the vertical-tangential plane. Due to the anisotropy of the swimmer, it rotates along its long axis that is in the plane of the dish (a detailed explanation is provided in the text). For quantitative studies we fixed the axis of rotation of the magnetic field with the use of three electromagnetic coils (inset (b)) that create a uniform magnetic field $\boldsymbol{H}$ rotating with frequency Ω in the (x, z) plane. The cartoons include a diagram showing the magnetic moment of the swimmer, $\boldsymbol{m}$, which follows the rotation of the field with frequency ω. For clarity the swimming object and the schematic of the coils disposition is not drawn to scale.

The general difficulty in exploiting a mechanism for moving objects based on the rotation of chiral structures in fluids may arguably be due to the limitations of techniques that are available for the fabrication of chiral shapes, particularly at the micron length scale. In contrast, the fabrication of planar objects with a wide range of length scales is both rapid and straightforward [34]. Our technique and its underlying physics are both scalable. In the rest of this report we describe swimming structures that are approximately 2 mm in length. As lithography allows for fabrication of smaller structures, this approach may provide one general mechanism for the design and fabrication of micron-scale structures that move autonomously.

We note that, in figure 1 we show the motion of swimmers that are forced to rotate by a rotating magnetic field produced by a magnetic stir plate (a rotating magnet, see figure 2(a)). The swimmers were immersed in a dish filled with fluid that was tall enough to accommodate their width but not their length. This constraint ensured that the long axis of the swimmers was approximately parallel to the plane of the stirrer. Although the magnetic field rotates mainly in the plane of the stirrer, there is also a small component of the field that rotates in the perpendicular plane. Interestingly, in this setup, the swimmers rotated about their long axis; this behavior (transmission of torque in the vertical plane, in spite of the fact that the main rotation of the field was in the horizontal plane) was caused by the anisotropy of the viscous drag coefficients for rotation about the long axis of the swimmer (smaller drag) and rotation about an axis perpendicular to the axis of the swimmer (larger drag). Although convenient for qualitative tests of motility of the elastic swimmers, the setup with the magnetic stir plate generates a non-uniform magnetic field and this non-uniformity introduces additional (to the hydrodynamic ones) forces on the swimmers. In order to characterize the motility of our swimmers quantitatively, in the rest of the paper we report experiments on a setup in which the rotating magnetic field is generated by three electromagnetic coils that created a rotating magnetic field of a uniform magnitude over an area in which we tested the speed of the swimmers.

2. Experimental details

2.1. Materials

PDMS elastomer base and curing agent were purchased from Dow Corning (Midland, MI). SU-8 2050 photoresist was from MicroChem (Newton, MA). Iron oxide nanoparticles (Starbond ferrite powder) was from Hoosier Magnetics. (Tridecafluoro-1,1,2,2-tetrahydrooctyl)-1-trichlorosilane was from Gelest (Morrisville, PA). Silicon wafers were from Silicon Sense (Nashua, NH). Transparency photomasks were printed at CadArt (Corvallis, OR). Ethylene glycol (density 1.3 g cm^{-3}, viscosity $\sim$16 mPa s) was from Sigma Aldrich and glycerine (density 1.3 g cm^{-3}, viscosity $\sim$1400 mPa s) was from Fluka.

2.2. Fabricating swimmers

We fabricated swimmers by microtransfer molding according to the procedure outlined in figure 3 [34, 35]. The process started with the fabrication of photoresist (SU8) structures. We used photolithography to transfer the design of the

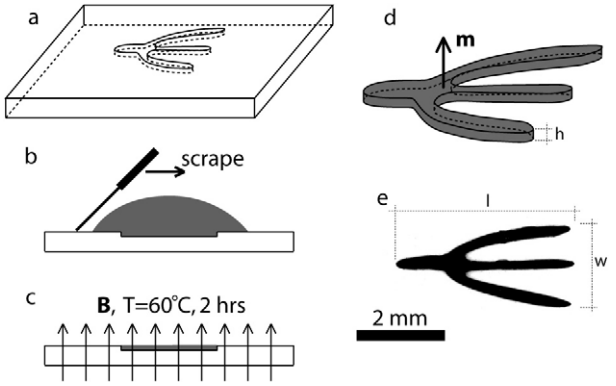

Figure 3. (a)–(c) A schematic diagram depicting the fabrication of the swimmers. (a) A PDMS mold embossed with the shape of a swimmer. (b) Indentations in the mold were filled with a mixture of PDMS prepolymer and ferromagnetic nanoparticles. (c) The polymer was cured thermally in the presence of an external magnetic field oriented perpendicularly to the plane of the swimmer. The arrows depict the direction of the field lines. (d) A cartoon of a swimmer that displays a net magnetic moment perpendicular to the plane of the swimmer with thickness, h. (e) An optical micrograph of a swimmer viewed from above.

swimmers from a transparency photomask into a layer of photoresist (SU8) that was spin-coated on the surface of a polished silicon wafer. The wafers were developed in propyleneglycol methylethylacrylate (PGMEA) to dissolve unexposed photoresist, leaving 'masters', which consisted of a wafer with photoresist structures in bas-relief. Masters were silanized by vapor phase deposition of (tridecafluoro-1,1,2,2-tetrahydrooctyl)-1-trichlorosilane for 3 h at 25 °C. The molds for fabricating swimmers were prepared by using masters to emboss the surface of slabs of PDMS. Specifically, we poured PDMS prepolymer—a 10:1 ratio of base to curing agent—on the wafer and cured it for 4 h at 65 °C. The molds were cut out with a scalpel, peeled away from the surface of the wafer, and trimmed. We treated the PDMS molds with an oxygen plasma to oxidize their surface and silanized them using a vapor phase deposition of (tridecafluoro-1,1,2,2-tetrahydrooctyl)-1-trichlorosilane for 3 h at 25 °C (figure 3(a)).

The indentations of the molds were filled with PDMS prepolymer (10:1, base to curing agent) admixed with ferrite powder (25% w/w) (figure 3(b)). Excess prepolymer/ferrite was scraped off the surface of the mold with a clean razor blade. The polymer was cured for 3 h at 60 °C with an external magnet positioned close to the mold so that the magnetic field was perpendicular to the surface of the mold (figure 3(c)). After the polymer was cured, the swimmers were carefully released from the mold with a pair of tweezers. This technique produced freestanding, planar, elastomeric swimmers with a magnetic dipole oriented perpendicular to the plane of their body. Typical dimensions for the swimmers varied between 2 and 10 mm long, 1–3 mm wide, and 100–200 μm thick; in principle it is possible to produce much smaller swimmers, although their release and manipulation becomes more difficult with decreasing dimensions. A schematic of a swimmer and a micrograph of its two-dimensional projection are depicted in figures 3(d) and (e).

2.3. Experiments with swimmers in a rotating magnetic field

An external magnetic field was created using three coils (figure 2(b)). Each coil had an inner diameter of 4 cm and an outer diameter of 7 cm and consisted of ∼1100 turns of 4 mm thin Cu wire. The magnetic field was rotated in the (x, z) plane, while (x, y) was the plane of the motion of the swimmers (see figure 2(b)). To produce a region of uniform magnetic field in the (x, y) plane, two coils were arranged in a Helmholtz configuration (e.g. placed on a common axis and separated by a distance equal to their radius). The coils were connected to a waveform generator (TTi TGA1244) that created the rotating magnetic field. The waveform generator was connected to a current amplifier (IMG STA-800). The intensity of the current flowing through the two perpendicular coil systems was adjusted so that the magnetic field rotated uniformly in the plane with a field constant amplitude $H = 10 \times 10^3$ or 11×10^3 A m^{-1} in the range of angular frequencies that we tested ($\Omega < 200$ s^{-1}). A teslameter (51662DE—Leybold, Germany) was used to measure the magnetic field intensity and its homogeneity.

PDMS swimmers were immersed in a Petri dish (3.7 cm diameter) filled with fluid mixtures (ethylene glycol: EG (1,2-ethanediol, Fluka), or a mixture of EG and glycerol) which spanned a range of viscosities from 16×10^{-3} to 0.3 Pa s and the dish was positioned above the z coil. We used tweezers to move the swimmers into the central region of the dish where the external magnetic field was uniform.

Videos were acquired using a CCD camera (Pixelink, PL-A741). By adjusting the settings for the camera we recorded images at ∼120 frames s^{-1} in a field of view that was ∼5 cm^2. An OM lens system (Olympus) with top illumination (Highlight 2001, Olympus) was connected to the camera with a C-mount adapter.

3. Results

3.1. Condition for the propulsion of objects rotating at low values of Re

At low values of Re, the force exerted on a fluid and the resulting flow are related linearly as described by the Stokes equations of motion: an inversion in the orientation of the force causes an inversion of the flow field. In this regime, streamlines can be reversed provided that the forces acting on the fluid have been reversed and are played 'backward' in time. Purcell's work shows that if the sequence of movements of an object (e.g. the movement of its limbs) possesses reciprocal symmetry, it does not result in a net flow of the fluid and the object produces no net motion. It follows that in order for a rotating object to display a rectified linear motion, the object, together with its axis of rotation must form a chiral structure. This can be satisfied either by a judicious choice of rotation of an appropriate static (and non-planar) shape that satisfies the above criterion, or via a rotation of an elastic shape that spontaneously deforms into a chiral shape (figures 4(a) and (b)).

The details of the mechanism of propulsion of a helix rotating at low Re are clearly illustrated in the movies created

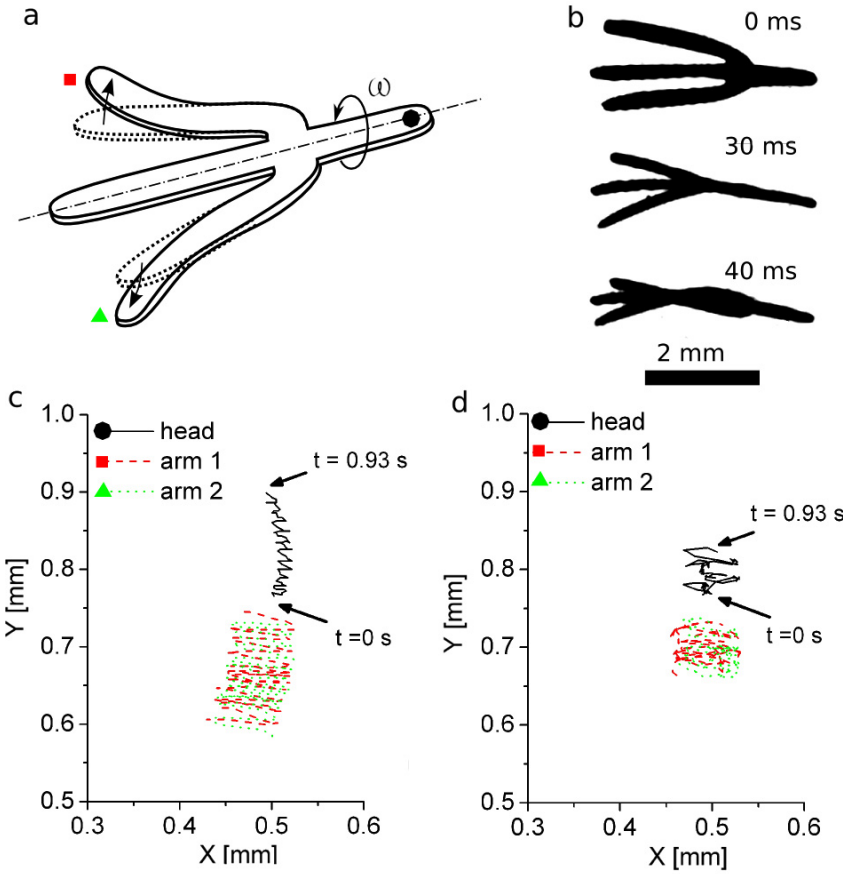

Figure 4. (a) A cartoon depicting a swimmer rotating around its long axis at a frequency ω. The arms of the swimmer deflect in the direction indicated by the arrows. The circle indicates the tip of the swimmer and the square and triangle indicate the ends of its two arms; we tracked each of these regions of the swimmer during our experiments. (b) Images of a swimmer deforming during one cycle of rotation ($\Omega = 6(2\pi)$ s^{-1}, in glycerine); the images were acquired on a stereoscope and brightness-contrast optimized with the use of Adobe Photoshop. (c) and (d) displacement of the tip (circle with the continuous line) and arms (squares with the dashed line and triangles with the dotted line) of the swimmer in an external magnetic field of intensity $H = 10 \times 10^3$ A m^{-1} and frequency $\Omega = 63$ s^{-1} (c) and $\Omega = 163$ s^{-1} (d).

by Taylor [36]. In summary, a helix can be divided into segments that are approximately cylindrical. A cylinder (or an oblique body) moving through a fluid experiences an anisotropic viscous drag. If the cylinder is dragged (forced) through a fluid at an angle relative to its long axis, the force F can be decomposed into two components that are parallel $F_\parallel$ and perpendicular $F_\perp$ to the length of the cylinder. Each of these components has to be balanced by the opposing viscous drag force $G_{\parallel/\perp} = -u_{\parallel/\perp}\eta a_{\parallel/\perp}$, where $u_{\parallel/\perp}$ is the speed of flow in the parallel ($\parallel$), and perpendicular ($\perp$) direction, η is the viscosity of the fluid, and $a_{\parallel/\perp}$ is the appropriate coefficient of drag. Since the parallel ($a_\parallel$) and perpendicular ($a_\perp$) drag coefficients are not equal, the ratio of the speeds $u_\parallel/u_\perp$ are not equal to the ratio of the forces $F_\parallel/F_\perp$, and as a result the net motion of the cylinder is not parallel to the applied force. A rotating helical object can be decomposed into cylindrical sections that are dragged (forced) in a direction perpendicular to the axis of rotation, but their speed is not perpendicular—it also consists of a component parallel to the axis of rotation. The lack of inversion symmetry guarantees that these 'parallel' contributions do not add up to zero. The result is that a rotating helical object creates a net flow of fluid along the axis of rotation and propels itself in the same direction and opposite orientation. Indeed, we observe that our swimmers rotating in a viscous fluid have a net displacement that is linear in time (figure 4(c)).

3.2. Synchronous rotation versus 'tumbling'

The designs of the swimmers that we analyzed consisted of a central 'body' that remains in the axis of rotation and two or more flexible arms that extend outward from the body. The viscous forces opposing the rotation of the swimmer deform it into a helical structure as illustrated in figures 4(a) and (b). The applied magnetic field rotates in the (x, z) plane with a frequency Ω and intensity $\boldsymbol{H}$, $\boldsymbol{H} = (H\cos(\Omega t), 0, H\sin(\Omega t))$. The magnetic torque $\boldsymbol{\tau}_\mathrm{m} \sim \boldsymbol{m} \times \boldsymbol{H}$ acting on the magnetic moment $\boldsymbol{m}$ of the swimmer forces it to follow the rotation of the field and, as a result, the swimmer rotates around its long axis with frequency ω and with both arms performing a circular motion around their common body.

When the swimmer rotates synchronously with the magnetic field ($\omega = \Omega$) it deforms into a shape that lacks the inversion symmetry, and translates through the fluid. An

example of the movement of a swimmer in a viscous fluid ($\eta = 16$ mPa s) is shown in figure 4(c), where the external magnetic field ($H = 10 \times 10^3$ A m^{-1}) was rotating at a frequency $\Omega = 63$ s^{-1}. A short version of the corresponding video is included in the supplementary information (available as video 2 at stacks.iop.org/JPhysCM/21/204110). In figure 4(c) we demonstrate the (x, y) positions of the tip of the swimmer as a function of time, and of the end points of the two arms that rotate around the main axis of the swimmer.

During rotation, the magnetic torque, $\boldsymbol{\tau}_{\mathrm{m}}$, is balanced by a viscous torque, $\boldsymbol{\tau}_{\mathrm{v}} \propto \eta\boldsymbol{\omega}$ that arises from the rotational motion of the swimmer in a fluid of viscosity η. From the balance of these torques and by considering a set of equations for the elastic deformation of each segment of the swimmer, one could, in principle, describe the dynamics of the arms during rotation. Due to the flexibility and to the complexity of the shape of the propeller, a detailed examination of this problem is computationally demanding, however not particularly illuminating and beyond the scope of this paper. The simplified approach that we take to analyze these objects assumes that the swimmer has a fixed magnetic moment $\boldsymbol{m}$; the magnitude of the magnetic torque $\boldsymbol{\tau}_{\mathrm{m}}$ depends only on the relative orientation of (the angle ϕ between) $\boldsymbol{m}$ and the magnetic field $\boldsymbol{H}$. The viscous torque $\boldsymbol{\tau}_{\mathrm{v}}$ increases linearly with the frequency ω of rotation of the swimmer. As long as the swimmer follows the rotation of the field synchronously, ϕ is constant. The value of ϕ increases with increasing ω in order for the magnetic and viscous torques to balance. For a given viscosity of the fluid, the strength of the magnetic field and the shape of the swimmer there is a critical rotational frequency Ω_{C} at which $\phi = \pi/2$, and above which ($\Omega > \Omega_{\mathrm{C}}$) the swimmer can no longer follow the rotation of the field synchronously. Indeed, we observe that for $\Omega > \Omega_{\mathrm{C}}$ the swimmer performs back-and-forth rotations (a rocking motion). A description of the dynamics of elongated objects that are permanently magnetized and are moving in response to external fields (asynchronous regimes) has been described for a number of systems, including: semiflexible filaments [37], ferromagnetic nano-rods [38], and elongated ferrofluid droplets [39]. The swimmer having two arms that are coupled dynamically also by dipolar interactions with the body complicate our system, however, the general behaviors of this transition can be reduced to these other examples.

The efficiency of swimming for $\Omega > \Omega_{\mathrm{C}}$ decreases with increasing Ω. This behavior is illustrated in figure 4(d) (see also video 3 in supporting information available at stacks.iop.org/JPhysCM/21/204110), where we show the trajectories of the arms and of the body of a swimmer subjected to a frequency $\Omega = 163$ s^{-1} ($\eta = 16$ mPa s, $H = 10 \times 10^3$ A m^{-1}). It is evident that the arms of the swimmer are 'trembling' and consequently motility is decreased. We refer to this mode of motion as 'tumbling' since it does not contribute to efficient translation and because it is *vaguely* reminiscent of the non-linear component of motion of cells of *E. coli* and other bacterial species during chemotaxis.

We characterized the propulsion of the swimmers by measuring their speed as a function of the frequency and the viscosity of the fluid. Figure 5 summarizes the results of these

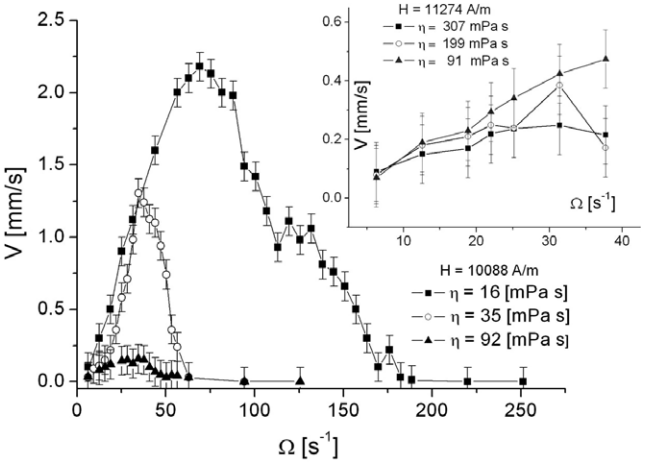

Figure 5. A plot of the velocity V versus external field frequency Ω of swimmers in an external magnetic field of intensity $H = 10 \times 10^3$ A m^{-1} and in fluid with different viscosities ($\eta = 16$, 35 and 92 mPa s). The plot inset shows the low frequency behavior of the velocity of swimmers in fluids with larger viscosities ($\eta = 91$, 199 and 307 mPa s) in a magnetic field of intensity $H = 11 \times 10^3$ A m^{-1}.

measurements for three values of viscosity: $\eta = 16$ mPa s (filled squares), 35 mPa s (open circles), and 92 mPa s (filled triangles) and at a fixed magnetic field strength ($H = 10 \times 10^3$ A m^{-1}). In all three cases, the velocity increased approximately linearly up to a maximum value (for example $V_{\mathrm{max}} = 2.2$ mm s^{-1} for $\eta = 16$ mPa s), and then decreased to zero at high frequencies ($\Omega > 170$ s^{-1} for $\eta = 16$ mPa s). We observed two distinct dynamic regimes: (i) in the first regime the velocity of the swimmers was linearly related to Ω; and (ii) in the second regime the velocity decreased with increasing Ω. The value (Ω_{C}) of the frequency of rotation of the field at which the behavior of the swimmer depends on viscosity of the medium: Ω_{C} decreased as η increases (e.g. $\Omega_{\mathrm{C}} = 68$ s^{-1} for $\eta = 16$ mPa s and $\Omega_{\mathrm{C}} = 34$ s^{-1} for $\eta = 92$ mPa s). In fact, the value of Ω_{C} follows well the theoretical prediction [37, 38]: $\Omega_{\mathrm{C}} \propto H/\eta$.

3.3. Speed of the swimmers

In accordance with the linearity of the Stokes equations, a rotating helix, or a rotating collection of angular, oblique bodies will achieve a net speed that is dependent only on the geometry of the object and on its rotational frequency, but not on the viscosity of the fluid it is immersed in. Similarly, the speed of the swimmers along the axis of their rotation should only be proportional to the linear speed of the rotating arms. In practice, the situation is more complicated for two reasons: (i) part of the swimmer's body remains in the axis of rotation where it does not contribute to the mechanism of propulsion and only introduces drag that opposes the net motion; and (ii) the shape of a swimmer depends on viscous torque, and is thus related to the viscosity of the solution. Point (i) introduces a drag that opposes the forward motion and that increases with increasing viscosity: causes the swimmers to move more slowly as the viscosity of the fluid increases. Point (ii) is

more difficult to analyze. We can assume that at low rotational speeds and low values of τ_v the deformation of a swimmer can be described by Hooks law and should be approximately proportional to τ_v. Since the deformation of the swimmer creates propulsion—at least at the smallest rotational speeds—the efficiency of motility should increase with an increase in structural deformation. As a consequence, we can expect that for a constant rotational frequency (ω) of the swimmer, swimmers immersed in higher viscosity fluids should translate more rapidly than those in lower viscosity fluids.

In our experiments we observe a slight decrease in the velocity of objects with increasing viscosity of the fluid (see the main graph and the inset in figure 5). Still, as the effect is small and lies within the experimental error of our measurements, it was difficult to verify experimentally the role and the relative importance of the aforementioned effects on the speed of the swimmers.

The relative ease of fabrication and testing of these flexible structures should make it possible for us to address the open question of what shape provides the highest efficiency of swimming at low *Re*. Here we describe the results of experiments with three variants of a geometry that is based on an elongated body that lies in the axis of rotation and two symmetric arms projecting outward from the swimmer. In addition to the tripod swimmer shown in figures 4 and 5, we also tested two designs with arms that were either longer (figure 6(a)) or shorter (figure 6(c)) than in the original design (figure 6(b)). The plot in figure 6 demonstrates the rectified speed of these designs as a function of the frequency of rotation of the field ($H = 11 \times 10^3$ A m^{-1}) at the same fluid viscosity ($\eta = 199$ mPa s). The results qualitatively confirm the assertion that the elastic deformation of the swimmers is critical for achieving a net displacement. The swimmer with the shortest arms achieved speeds that are negligibly smaller than the two other designs (see video 4 in supporting information available at stacks.iop.org/JPhysCM/21/204110). The swimmer with the longest arms, which we anticipate will bend and deform more at the same or similar frequency of rotation, translates through fluid the fastest (see video 4 in supporting information available at stacks.iop.org/JPhysCM/21/204110). The swimmer with the longer arms reached a speed 0.6 mm s^{-1} at $\Omega \sim 40$ s^{-1} which was two times larger than the maximum speed of our basic design ($\sim$0.3 mm s^{-1} at $\Omega \sim 25$ s^{-1}).

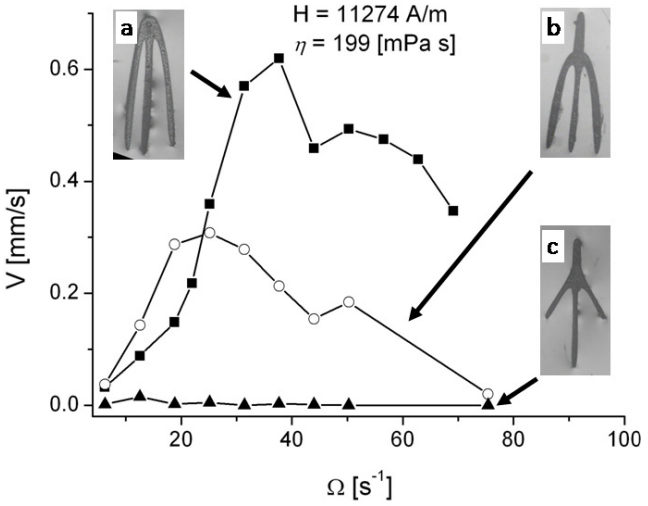

Figure 6. A plot of the speed versus frequency of rotation for three different designs of elastic swimmers: (a) a swimmer with long arms, (b) the swimmer described in the paper, and (c) a swimmer with short arms.

4. Discussion

4.1. Dynamic structures

Many microorganisms translate through fluids using flagella and cilia. These mechanisms involve the rotation of flexible organelles (e.g. flagella) that have a shape that is deformed during their motion. For example, the flagella on cells of *E. coli* are flexible [40] and their helicity is visibly distorted when a stress is placed on the flagella, such as when the direction of flagellar motors is reversed. Arguably, bacteria and other microorganisms that swim at low *Re* have adapted to these conditions and solved the optimization problem of how to deform static structures into dynamic, helical rotors.

Purcell demonstrated that the efficiency of propulsion using a rotating object may be maximized by adjusting two parameters: (1) matching the size of the rotor to the size of the propelled object; and (2) designing an appropriately shaped rotor [3]. The first parameter may be satisfied relatively easily while satisfying the second is very difficult. In fluid dynamics, the search for optimal geometries is usually performed empirically through numerical simulation or by experiment. In the case of deformable bodies the problem is even more difficult, as one has to solve both for the flow field around a body and for the simultaneous deformation of the body—thus the problem has to be rephrased from 'which propeller shape is most efficient for propulsion?' to 'what structure will become *deformed* into a propeller shape that is most efficient for propulsion?' Our system provides an experimental platform for studying this optimization problem and related questions and will make it possible to iteratively test self-propelled structures for motility at low *Re*, and test the dependence of the efficiency of propulsion as a function of the elastic constant (Young modulus) of the material from which the swimmers are fabricated. These studies may provide insight into the shapes of motile microorganisms and their efficiency and the extent to which nature has explored motility 'phase space' to optimize solutions to this problem. Because the structures are planar and are fabricated using photolithography it is also possible that an optimized shape could be scaled down to dimensions of tens of microns (instead of millimeters). Such downscaling should only ensure that the Reynolds number of the flow is small and that the mechanism of propulsion by rotation of a chiral object is a proper choice. A potential problem is hidden in the proper choice of a material and of the Young modulus. One other potential point that should be considered—and was not addressed in this report—when studying the propulsion of micron-scale elastic swimmers is the effect of fluctuations in the flow.

4.2. Uniformity of the magnetic field

One inconvenient aspect of using magnetic fields to rotate elastic swimmers is that this mechanism requires regions of uniform magnetic field, which at the current length scale of the swimmers is difficult to achieve. One approach to overcome this problem is to use a larger size ratio of the magnet to the swimmer. The use of rotating magnetic field for the control of propulsion of the elastic rotary swimmers has the advantage that their speed and direction of motion can be continuously and precisely controlled.

5. Conclusions

In this paper we demonstrate the movement of planar magnetized and elastic objects immersed in a fluid and subjected to a rotating magnetic field. These objects rotate around their long axis; the resulting viscous drag deforms the swimmers into three-dimensional, helical objects. The deformed structures translate through fluids in a direction parallel to the long axis of their body. This technique has the useful characteristic that it transmits torque without mechanical contact, and may provide a useful tool for studying the correlation between the shape of a deformable swimming object and its velocity. Our technique for fabricating deformable swimmers is simple and makes possible the study of finding the optimal shape of a deformable swimmer that uses rotation as a means for propulsion.

Acknowledgments

Project co-operated within the Foundation for Polish Science Team Programme co-financed by the EU European Regional Development Fund. PG acknowledges support from the Foundation for Polish Science under the Homing program. DBW acknowledges support from the Searle Scholar Foundation and 3M Inc. PT was supported by the program 'Beatriu de Pinós' BP-B100167. FS and PT acknowledge financial support by MEC (Project FIS2006-03525) and DURSI (2005SGR00653), GMW acknowledges support from the US DOE Grant DE-FG02-00ER45852.

References

[1] Taylor G I 1951 *Proc. R. Soc.* A **209** 447
[2] Taylor G I 1952 *Proc. R. Soc.* A **211** 225
[3] Purcell E M 1977 *Am. J. Phys.* **45** 3
[4] Berg H C 1993 *Random Walks in Biology* (Princeton, NJ: Princeton University Press) p 75
[5] Bray D 2000 *Cell Movements: from Molecules to Motility* (New York: Garland) p 257
[6] Happel J and Brenner H 1973 *Low Reynolds Number Hydrodynamics* (Leiden: Noordhoff)
[7] Berg H C 2003 *Annu. Rev. Biochem.* **72** 19
[8] DiLuzio W R, Turner L, Mayer M, Garstecki P, Weibel D B, Berg H C and Whitesides G M 2005 *Nature* **435** 1271
[9] Lauga E, DiLuzio W R, Whitesides G M and Stone H A 2006 *Biophys. J.* **90** 400
[10] Berke A P, Turner L, Berg H C and Lauga E 2008 *Phys. Rev. Lett.* **101** 038102
[11] Becker L E, Koehler S A and Stone H A 2003 *J. Fluid Mech.* **490** 15
[12] Qian B, Powers T R and Breuer K S 2008 *Phys. Rev. Lett.* **100** 078101
[13] Kim M, Bird J C, Van Parys A J, Breuer K S and Powers T R 2003 *Proc. Natl Acad. Sci. USA* **100** 15481
[14] Paxton W F, Kistler C K, Olmeda C C, Sen A, Angelo S K St, Cao Y, Mallouk T E, Lammert P E and Vincent H C 2004 *J. Am. Chem. Soc.* **126** 13424–31
[15] Dhar P, Cao Y, Kline T, Pal P, Swayne C, Fischer T M, Miller B, Mallouk T E, Sen A and Johansen T H 2007 *J. Phys. Chem.* C **111** 3607
[16] Dreyfus R, Baudry J, Roper M L, Fermigier M, Stone H A and Bibette J 2005 *Nature* **437** 862
[17] Howse J R, Jones R A, Ryan A J, Gough T, Vafabakhsh R and Golestanian R 2007 *Phys. Rev. Lett.* **99** 048102
[18] Tierno P, Golestanian R, Pagonabarraga I and Sagués F 2008 *Phys. Rev. Lett.* **101** 218304
[19] Chang S T, Paunov V N, Petsev D N and Velev O D 2007 *Nat. Mater.* **6** 235
[20] Ogrin F Y, Petrov P G and Winlove C P 2008 *Phys. Rev. Lett.* **100** 218102
[21] Ismagilov R F, Schwartz A, Bowden N and Whitesides G M 2002 *Angew. Chem. Int. Edn* **41** 652
[22] Agrawal A, Kanti Dey K, Paul A, Basu S and Chattopadhyay A 2008 *J. Phys. Chem.* C **112** 2797
[23] Laocharoensuk R, Burdick J and Wang J 2008 *ACS Nano* **2** 1069
[24] Paxton W F, Baker P T, Kline T R, Wang Y, Mallouk T E and Sen A 2006 *J. Am. Chem. Soc.* **128** 14881
[25] Wang F Y, Hernandez R M, Barlett D J Jr, Bingham J M, Kline T R, Sen A and Mallouk T E 2006 *Langmuir* **22** 10451
[26] Sundararajan G S, Lammert P E, Zudans A W, Crespi V H and Sen A 2008 *Nano Lett.* **8** 1271
[27] Qin L, Banholzer M J, Xu X, Huang L and Mirkin C A 2007 *J. Am Chem. Soc.* **129** 14870
[28] Stock C, Heureux N, Browne W R and Feringa B 2007 *Chem. Eur. J.* **14** 3146
[29] Hiratsuka Y, Miyata M and Uyeda T Q P 2005 *Biochem. Biophys. Res. Commun.* **331** 318
[30] Hiratsuka Y, Miyata M, Tada T and Uyeda T Q P 2006 *Proc. Natl Acad. Sci. USA* **103** 13618
[31] Darnton N, Turner L, Breuer K and Berg H C 2004 *Biophys. J.* **86** 1863
[32] Weibel D B, Garstecki P, Ryan D, DiLuzio W R, Mayer M, Seto J F and Whitesides G M 2005 *Proc. Natl Acad. Sci. USA* **102** 11963
[33] Behkam B and Sitti M 2007 *Appl. Phys. Lett.* **90** 023902
[34] Xia Y and Whitesides G M 1998 *Angew. Chem. Int. Edn* **37** 550
[35] Zhao X-M, Xia Y and Whitesides G M 1996 *Adv. Mater.* **8** 837
[36] Taylor G I 1961 Low Reynolds number flow *Series of Educational Movies in Fluid Dynamics by the National Committee for Fluid Mechanics Films* http://web.mit.edu/hml/ncfmf.html
[37] Keshoju K, Xing H and Suna L 2007 *Appl. Phys. Lett.* **91** 123114
[38] Belovs M and Cebers A 2006 *Phys. Rev.* E **73** 051503
[39] Lacis S, Bacri J C, Cebers A and Perzynski R 1997 *Phys. Rev.* E **55** 2640
[40] Darnton N C and Berg H C 2007 *Biophys. J.* **92** 2230